

Deterministic Model for the Analysis of YALINA-Booster Experiments with the ERANOS Code System

G. Aliberti ¹, Y. Gohar ¹, F. Kondev ¹, A. Talamo ¹, H. Kiyavitskaya ², V. Bournos ², Y. Fokov ², C. Routkovskaya ², I. Serafimovich ²

¹ Argonne National Laboratory, 9700 South Cass Avenue, Argonne, IL 60439, USA

² JIPNR-Sosny, National Academy of Sciences, acad. Krasin, 99. 220109, Minsk, Belarus

Email contact of main author: aliberti@anl.gov

Abstract. An experimental program has been launched by the Joint Institute for Power and Nuclear Research – Sosny (JIPNR-Sosny), National Academy of Sciences of Belarus with the purpose to study the physics of Accelerator Driven Systems. This paper gives an overview of the analysis of YALINA-Booster and it provides a detailed description of the adopted approach to create a calculational model based on the use of a deterministic code.

1. Introduction

The growing stockpile of nuclear waste constitutes a severe challenge for the mankind during the coming hundred thousands years. To reduce the radiotoxicity of the nuclear waste, the Accelerator Driven System (ADS) has been proposed [1]. One of the most important problems of ADSs technology is the choice of the appropriate neutron spectra for the transmutation of Minor Actinides (MA) and Long Lived Fission Products (LLFP). In this context, the YALINA experimental program [2] is currently underway at the JIPNR-Sosny center in Belarus.

2. YALINA-Booster Facility

YALINA-Booster [3] has been designed to have both fast and thermal neutron spectra in one configuration. The subcritical assembly is driven by an external neutron source: a Cf-252 neutron source or a deuteron accelerator with deuterium or tritium targets for (d,d) or (d,t) neutron production. YALINA-Booster (*see FIGs.1. and 2.*) has a central fast neutron zone surrounded by a thermal neutron zone. The fast (“booster”) zone multiplies the external neutrons through the fission reactions of highly enriched uranium (HEU) and (n,xn) reactions of lead. The produced neutrons leak to the surrounding thermal zone. Between the two zones, there is an interface, called “valve” zone, consisting of two layers: the inner layer has metallic natural uranium rods (*see FIG.3.*) and the outer layer has boron carbide rods (*see FIG.3.*) that absorb thermal neutrons. Such “valve” zone enables fast neutrons to penetrate into the thermal zone and prevents thermal neutrons from entering the booster zone from the thermal zone.

The fast booster zone consists of 36 lead subassemblies. The thermal zone consists of 108 polyethylene subassemblies, loaded with EK-10 fuel rods (UO₂ fuel rods with 10% U-235 enrichment, UO₂-10%, *see FIG.3.*). A different number of EK-10 fuel rods can be loaded to achieve different subcriticality levels: the configuration considered in this paper corresponds to a loading of 1141 EK-10 rods (YALINA-Booster 1141).

For structural reasons, the subassembly has a stainless steel frame, which divides the assembly to 16 frames. Each frame has nine subassemblies. Cutting out the four corners of the four frames at the assembly center creates a hole (*see FIG.1.*) to host a lead target for one half axial extension and the beam tube for the other half (*see FIG.2.*). The inner part of the fast zone, surrounding the lead target, contains 132 metallic uranium rods (*see FIG.3.*) with 90% U-235

then used to perform reactivity and flux calculations. In the VARIANT code, the transport equation is derived in terms of an “even” and an “odd” flux, expanded in Legendre’s polynomials and in spherical harmonics for the spatial and angular variables respectively, as shown in the following equations:

$$\Phi_S^+(\vec{r}, \vec{\Omega}) = \frac{1}{2} [\Phi_S(\vec{r}, \vec{\Omega}) + \Phi_S(\vec{r}, -\vec{\Omega})] = \sum_{i,m} f_i(\vec{r}) g_m(\vec{\Omega}) \zeta_{i,m} \quad \text{Eq. 1}$$

$$\Phi_{S,\gamma}^-(\vec{r}, \vec{\Omega}) = \frac{1}{2} [\Phi_S(\vec{r}, \vec{\Omega}) - \Phi_S(\vec{r}, -\vec{\Omega})] = \sum_{j,n} h_j(\vec{r}) k_n(\vec{\Omega}) \chi_{j,n,\gamma} \quad \text{Eq. 2}$$

VARIANT uses the nodal variational method. This implies that the solution of the neutron equation is integrated over the volume of the meshes and it is obtained by the minimization of a function, which contains the total cross-section (Σ_t) at the denominator. Due to these features, the VARIANT code does not work properly with fine meshes. Moreover, difficulties are encountered in presence of void regions, characterized by low values of Σ_t and, as consequence, the existing empty spaces in the original YALINA-Booster configurations had to be homogenized with other materials.

In summary, with the use of a deterministic code system like ERANOS, local effects cannot be explicitly simulated. Therefore, a physical approach is required to correctly reproduce the global effects in the selected regions where the cross-sections are processed, so that the results can be obtained without any loss of accuracy.

4. Cross-Section Processing

The cross-sections have been processed with the ECCO code using the nuclear data from the JEF2.2, JEF3.1 and ENDF/B-VI.8 libraries. The cell calculations are performed separately for each region assumed to be infinite. The ECCO code utilizes the sub-group method for the treatment of the resonances and allows to perform cell calculations in homogeneous (0D) and heterogeneous geometries (1D: cylindrical, slab; 2D: XY, hexagonal), based on the collision probability method. The cross-sections are first calculated over a fine energy group structure (up to 1968 energy groups) then are collapsed to a broader energy group structure using the cell flux as weighting function. For the present work, the condensation has been performed over the standard 172 group structure often used for the analysis of nuclear reactors with deterministic codes. However, deterministic calculations for reactivity or neutron flux determination of the YALINA-Booster configurations with 172 energy groups require significant computational resources, computer memory and computational time. As consequence, the cross-sections have been also processed with a lower number of energy groups. For this purpose, a 53 energy group structure was derived from the standard 33 group structure used for fast reactor analysis: two groups have been added at high energy in order to represent the 14 MeV (d,t) source; then, at low energy, the 3 last energy groups from the original 33 group structure have been replaced by 20 energy groups for a more appropriate treatment of the neutron slowing down in the thermal zone (see Table I).

In heterogeneous geometry, after condensation the cross-sections are homogenized over the cell volume. For non-fissile (structural) media, the cell flux is calculated by introducing a source term given by the neutron leakage from the neighbouring cell. This term is DB^2 , where D is the diffusion coefficient and B the value of the buckling driving the leakage, specified by the user. In absence of specific information, in the present study B^2 has been fixed to 0 for all subcritical medium calculations. However, the dependence of the results on possible different values provided for the buckling has been investigated and the results indicated a quite negligible impact.

TABLE I: 53 ENERGY GROUP STRUCTURE.

Gr.	Energy ^(a)										
1	1.964E+1	10	4.979E-1	19	5.531E-3	28	6.790E-5	37	9.100E-7	46	2.480E-7
2	1.419E+1	11	3.020E-1	20	3.355E-3	29	4.017E-5	38	8.500E-7	47	1.600E-7
3	1.396E+1	12	1.832E-1	21	2.035E-3	30	2.260E-5	39	7.900E-7	48	1.400E-7
4	1.000E+1	13	1.111E-1	22	1.234E-3	31	1.371E-5	40	7.050E-7	49	1.000E-7
5	6.065E+0	14	6.738E-2	23	7.485E-4	32	8.315E-6	41	6.250E-7	50	5.000E-8
6	3.679E+0	15	4.087E-2	24	4.540E-4	33	4.000E-6	42	5.400E-7	51	3.500E-8
7	2.231E+0	16	2.479E-2	25	3.043E-4	34	2.768E-6	43	4.850E-7	52	2.500E-8
8	1.353E+0	17	1.503E-2	26	1.486E-4	35	1.370E-6	44	4.330E-7	53	1.500E-8
9	8.209E-1	18	9.119E-3	27	9.166E-5	36	9.500E-7	45	3.200E-7		

^(a) Upper Energy boundary [MeV]. In bold are the energy boundaries of the original 33 group structure.

4. 1. Cell Calculation Scheme for the Thermal Zone

Particular interest has been devoted to the calculation of the thermal cells. In fact, the ERANOS code system was initially developed for the analysis of fast systems, but since it also has extended capabilities for the treatment of the neutron slowing down with up to 1968 energy groups, it can be also used for the analysis of thermal systems.

In order to investigate the ERANOS performances when calculating thermal systems, calculations have been performed for the single pin loaded in the thermal zone (see figure in Table II) and the obtained results have been compared with MCNPX. The pin is assumed to be infinite in the axial direction (2D calculation) with reflection boundary conditions in X and Y. The results for k_{inf} (see Table II) and flux spectra (*see FIG.4.*) demonstrated an excellent agreement between ERANOS and MCNPX if the polyethylene region is subdivided in an appropriate number of subregions. Table II also shows that the spatial self-shielding in the fuel pin does not play an important role: using three subregions for the fuel pin produces practically the same results than using a single region.

Based on the results of the present investigation, the polyethylene regions of all cell configurations for the cross-section processing of YALINA-Booster have been accurately subdivided in an appropriate number of subregions. For similarity, all other material regions (fuel, lead, etc.) in the cell configurations, have been also subdivided in an opportune number of subregions, to take into account the self-shielding or spatial effects.

TABLE II: YALINA THERMAL PIN: ERANOS k_{inf} VALUES.
(k_{eff} VALUE WITH MCNPX USING ENDF/B-VI.6 DATA IS 1.36510 ± 0.00012).

	Regions (n. of Subregions)		ERANOS - ENDF/B-VI.8: k_{inf}
	Fuel (1); Poly (1)		1.379933
	Fuel (3); Poly (7) ^(*)		1.363473
	Fuel (1); Poly (7)		1.363471

^(*) Flux spectra of this case are represented in Fig.4.

4. 2. Detailed Description of the YALINA-Booster Deterministic Model

The deterministic model derived for YALINA-Booster is shown in *FIGs.5. and 6.* for the axial and XY layouts respectively. *FIGs.5. and 6.* show the zones used for generating cross-section sets: e.g., a homogeneous set of cross-section is associated with a zone number. The zones containing the experimental channels (not shown in *FIG.5.*) are also considered and in total 113

cell calculations were performed to describe the deterministic model of YALINA-Booster 1141.

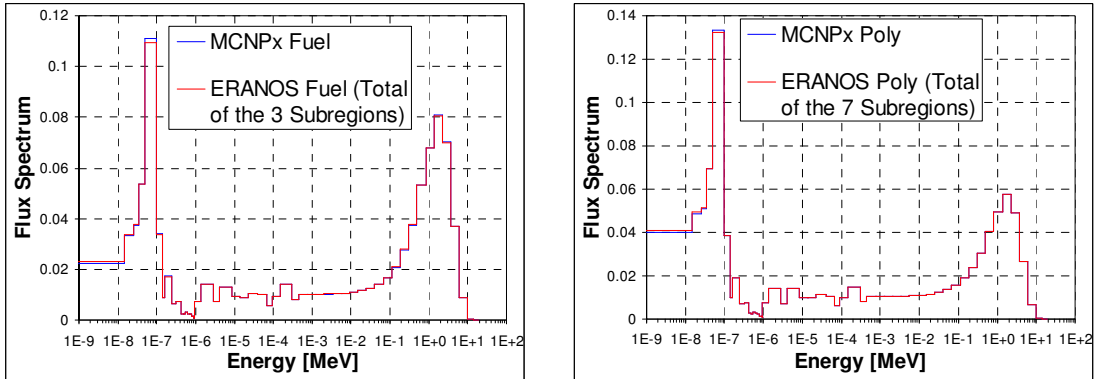
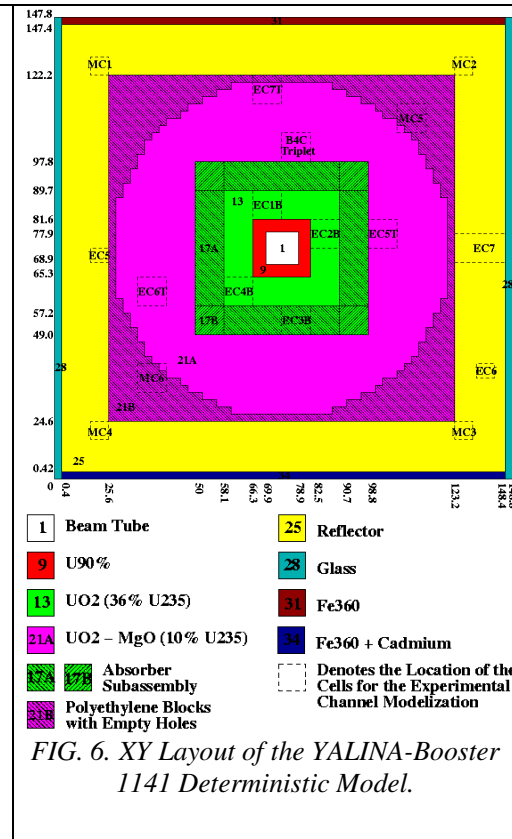
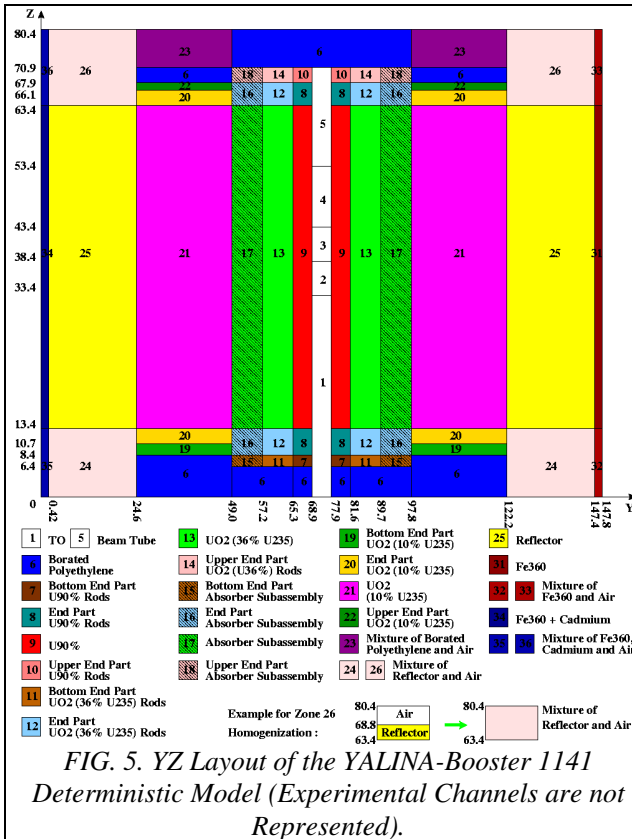


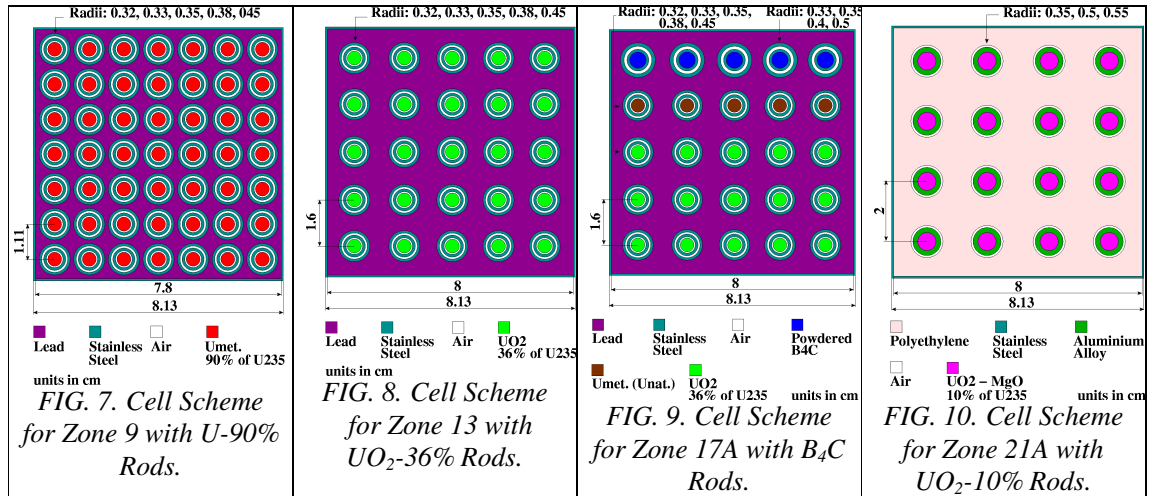
FIG. 4. MCNPX-ERANOS Flux Spectra Comparison.



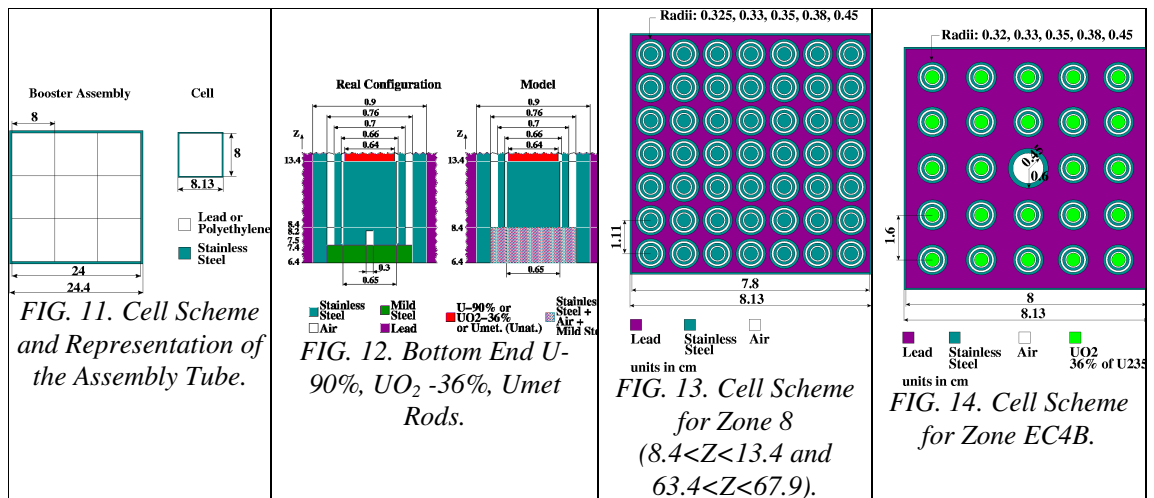
As explained before (see Section 3), due to the code difficulties to explicitly model void regions, void zones of the YALINA-Booster configurations had to be homogenized with other materials. For instance, zones 24 and 26 have been obtained by the homogenization of reflector (essentially graphite) and air (as indicated in FIG.5.). Similarly, zone 23 is the result of a homogenization between the borated polyethylene blocks and air. Additional homogenizations have been performed for the representation of the end part of the fuel rods and of the experimental channels (details will be discussed later). In the YALINA-Booster configurations, heterogeneity effects are very important, therefore the cross-sections of most of the regions have been processed with a XY heterogeneous cell

calculation. Generally, the cell is chosen with the purpose to represent the XY cut of the lead or polyethylene blocks (see e.g. cell description of the fuel zones in FIGs.7. to 10.). In these figures, it can be noticed that each cell is surrounded by a stainless steel frame. In the YALINA-Booster assembly, the stainless steel frame surrounds nine cells (see FIG.11.), therefore this stainless steel is equally subdivided per each cell (polyethylene or lead).

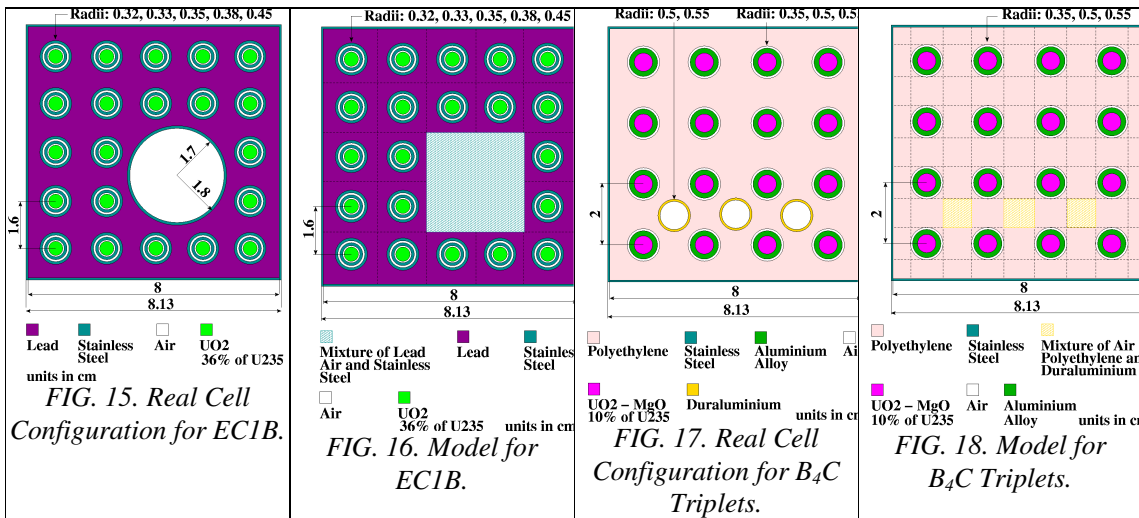
A particular attention has been devoted to the absorber subassemblies with the B₄C rods. For these zones, the cross-sections have been processed according to the scheme indicated in FIG.9. and the cell calculations have been performed as for subcritical media with the leakage from the thermal zone.



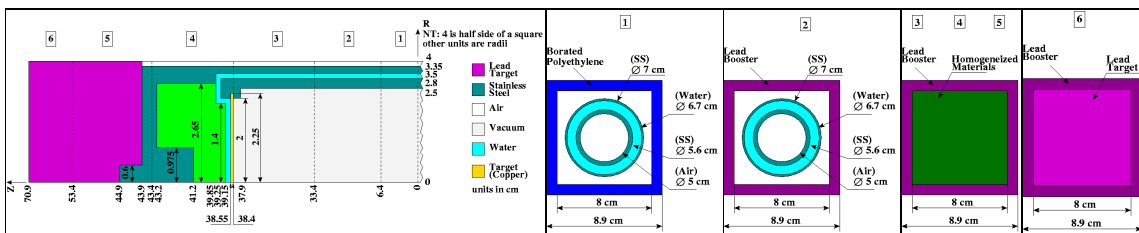
The axial meshes were chosen (see FIG.5.) to match the fuel rods geometry of FIG.3. at Z = 6.4, 8.4, and 13.4 cm (see FIG.12.). For these regions, the cross-sections have also been represented in heterogeneous geometry, as described in FIG.13. However, for some zones a homogenization of the materials had to be made, as indicated in FIG.12. Similar considerations apply to the top end of the fuel rods at Z = 63.4, and 70.9 cm; the bottom end of the B₄C rods at Z = 6.4 and 13.4 cm; the top end of B₄C rods at Z = 63.4, and 70.9 cm; the bottom end of EK-10 rods at Z = 8.4, and 13.4 cm; and the top end of EK-10 rods at Z = 63.4 and 67.9 cm.



For the borated polyethylene and reflector regions, cross-sections have been processed with a homogeneous cell calculation, after homogenization of the materials. In order to avoid the presence of explicit void regions and fine meshes in the deterministic model, the experimental channels are accurately homogenized with the region (or part of it) where they are located. As consequence, the experimental channels located in the reflector are homogenized with an opportune volume of the reflector itself. The experimental channels located in the fuel regions are homogenized over the volume of the cell used to create the cross-section for the fuel region where they are located (see e.g. FIG.14. for the cell scheme adopted for the experimental channel EC4B). Additionally, due to the limitations imposed by the cell code in the geometry description, some simplification had to be adopted in order to describe the presence of the experimental channels consistently with the cell lattice used for the description of the other pins. For instance, FIG.15. shows the real geometry description of the cell containing the experimental channel EC1B, while FIG.16. shows the model. Similarly, FIGs.17. and 18. show the solution adopted to represent the B₄C channels in the thermal zone.



The central subassembly of YALINA-Booster, containing both the duct and the target of the deuteron beam, has been represented in 6 axial zones, according to the representation of FIG.19. The XY layout of the cells used for the cross-section processing is also shown in FIG.19. for each axial zone. It can be observed that the geometrical layout of these cells includes part of the lead material outside the beam duct/target. This lead corresponds to the gap between the three rings of the U-90% rods (the pitch between the rods is 1.14 cm) and the section of the lead target (8x8 cm). To avoid the introduction of fine meshes in the deterministic model, it is decided to homogenize the cross-sections of this lead area together with the beam duct/target in a single cell calculation in a heterogeneous geometry, as represented in FIG.19.



5. YALINA-Booster Calculation Results and Conclusions

For the YALINA-Booster configurations, calculations have been performed for the multiplication factor, the source multiplication factor, flux spectra, reaction rates along selected experimental channels, kinetic parameters (effective fraction of delayed neutrons and mean generation time) and kinetic studies of the time response of the subcritical system to a short ($5\mu\text{s}$ wide) neutron pulse of the external source. The obtained calculations have been also compared to the experiment and in general the agreement has been found quite satisfactory. Table III shows the comparison of the calculated and experimental reactivities values. FIGs.20. and 21. show an example of comparison for reaction rate traverses and dynamic response to a (d,d) neutron pulse. The present study demonstrates the successful utilization of the deterministic method using ERANOS code system to analyze the complicated configuration of the YALINA-Booster experiment.

TABLE III: CALCULATED AND MEASURED k_{eff} (REACTIVITY) FOR YALINA-BOOSTER.

Number of EK-10 rods	JEF2.2	JEF3.1	ENDF/B-VI.8	Measurements (*) in
Booster 1141	0.976162 (-2442 pcm)	0.973028 (-2772 pcm)	0.972233 (-2856 pcm)	EC5T, EC6T, EC7T: 0.973236 (-2750 pcm)
Booster 902	0.939629 (-6425 pcm)	0.932845 (-7199 pcm)	0.932305 (-7261 pcm)	EC6T: 0.931099 (-7400 pcm)

(*) Performed by area ratio method and corrected with Bell and Glasstone spatial correction factors.

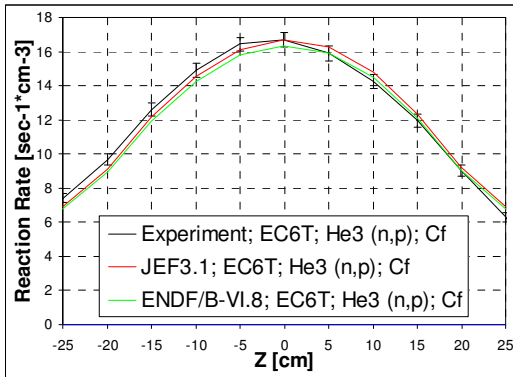


FIG. 20. He-3 (n,p) Distribution in EC6T of YALINA-Booster 1141.

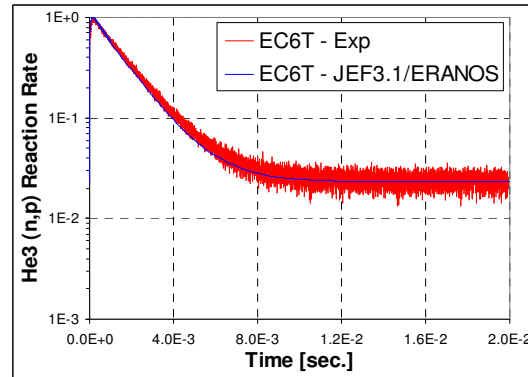


FIG. 21. He-3 (n,p) Response to a (d,d) Pulse in EC6T of YALINA-Booster 1141.

Acknowledgments

Argonne National Laboratory's work is supported by the U.S. Department of Energy, National Nuclear Security Administration, Office of Global Nuclear Material Threat Reduction (NA213).

References

- [1] SALVATORES, M. et al., "Long-lived, radioactive waste transmutation and the role of accelerator driven (hybrid) systems," Nuclear Instruments and Methods in Physics Research, A 414 5-20 (1998).

- [2] CHIGRINOV, S.E et al., Experimental Investigations on Neutronics of the Accelerator Driven Transmutation Technologies at the Subcritical Facility “YALINA” Proceedings of the ANA/ADTTA, Reno, Nevada, 11-15 November 2001.
- [3] BOURNOS, V. et al., “YALINA-Booster Benchmark Specifications for the IAEA Coordinated Research Projects on Analytical and Experimental Benchmark Analysis on Accelerator Driven Systems, and Low Enriched Uranium Fuel Utilization in Accelerator Driven Sub-Critical Assembly Systems,” February 2007.
- [4] RIMPAULT, G. et al., The ERANOS Code and Data System for Fast Reactor Neutronic Analyses, in Proceedings of PHYSOR 2002 Conference, Seoul, South Korea, October 2002.
- [5] RIMPAULT, G. “Algorithmic Features of the ECCO Cell Code for treating Heterogeneous Fast Reactor Assemblies,” International Topical Meeting on Reactor Physics and Computation, Portland - Oregon, May 1-5, 1995.
- [6] PALMIOTTI, G., CARRICO, C.B. and LEWIS, E.E. "Variational Nodal Transport Methods with Anisotropic Scattering," Nucl. Sc. Eng., 115, p.233 (1993).